DALTON

X-Ray absorption fine structure study of the structural changes accompanying spin cross-over in the acetone solvates of $[Fe(dppen)_2X_2]$ [dppen = *cis*-1,2-bis(diphenylphosphino)ethylene; X = Cl or Br]*

Nigel A. Young

School of Chemistry, University of Hull, Hull HU6 7RX, UK

Iron and bromine K-edge X-ray absorption fine structure (XAFS) have been used to determine the changes in the local iron environment in $[Fe(dppen)_2Br_2]\cdot 2Me_2CO$ on going through the spin cross-over transition at 160–185 K. The mean Fe–P bond length decreases from the high- to the low-spin isomer by 0.29 Å [2.60(3) to 2.31(3) Å], whereas the mean Fe–Br bond length decreases by only *ca.* 0.02 Å [2.51(3) to 2.48(3), iron K-edge; 2.48(3) to 2.47(3) Å, bromine K-edge]. Iron K-edge XAFS for $[Fe(dppen)_2Cl_2]\cdot 2Me_2CO$ showed a reduction of 0.28 Å in the mean Fe–P distance [2.55(3) to 2.27(3) Å] and a reduction of 0.02 Å in the mean Fe–Cl bond length [2.33(3) to 2.31(3) Å] on going from the high- to the low-spin form, in good agreement with literature values, the spin transition being observed at 220–240 K.

The phenomena of spin cross-over in (pseudo) octahedral first-row transition-metal complexes with a d^4, d^5, d^6 or d^7 electronic configuration induced by a change in either temperature or pressure has been known for a long time;[1] more recently such processes have been suggested for possible data-storage media.[2] It is also possible to induce the spin transition photochemically using the techniques variously called LIESST[3] (light-induced excited spin-state trapping), STEPS[4] (susceptibility of transient excited paramagnetic states), or LD-LISC[5] (ligand-driven light-induced spin changes). The change from high spin (spin free) to low spin (spin paired) is accompanied by a formal decrease in antibonding electron density and a rise in non-bonding electron density (assuming σ bonding only). This is often accompanied by a change in the local co-ordination environment of the metal, usually being manifested as shorter metal–ligand bond lengths in the low-spin complexes.

The classical approach to determining the structural changes occurring during spin cross-over is to use single-crystal X-ray diffraction.[6] Whilst this is a very powerful technique there are some severe problems in using it for this type of experiment, not the least being that the structural changes can often lead to severe lattice strain in the crystal, which leads to a loss in diffracted intensity. It is also usually necessary to carry out at least two determinations, one above the transition point (usually ambient) and one below it, often at around 100 K. There are, however, an increasing number of reports on the use of variable-temperature[7] or variable-pressure single crystal diffraction[8] to study the structural changes occurring during spin cross-over. Powder diffraction[6] is able to determine changes in the space group and lattice parameters, and identify whether a phase change occurs during spin cross-over, but is not usually able to yield values of the metal–ligand bond lengths.

X-Ray absorption fine-structure spectroscopy (XAFS)[9] is a powerful probe of the *local* structure of the element under investigation, and is independent of the phase or long-range order of the material. Therefore, it is ideally suited to the study of structural changes during spin cross-over as these occur predominantly within the metal local co-ordination environment. Metal K-edge XAFS has been used to study the structural and electronic changes occurring during spin cross-over in iron(II) complexes,[10] iron haem model compounds,[11] iron(III) complexes[12] and cobalt(II) complexes.[13] Additionally there are a few reports of the use of iron L-edge[10e,14] and cobalt L-edge[15] XAFS to investigate changes in electronic structure.

The systems chosen for this study were the acetone solvates of $[Fe^{II}(dppen)_2X_2]$ (dppen = *cis*-1,2-bis(diphenylphosphino)-ethylene; X = Cl or Br) as these are relatively little studied compared to the N-donor iron(II) systems and appear to be the only well established examples of spin cross-over in iron(II) phosphine complexes. Levason *et al.*[16] first observed anomalous behaviour in the magnetic and Mössbauer data for $[Fe(dppen)_2Cl_2]$, indicating that it was undergoing a gradual spin cross-over with the high-spin proportion being 90, 81 and 62% at 293, 195 and 83 K respectively. They found that $[Fe(dppen)_2Br_2]$ was high spin at all the temperatures studied (360–90 K). Cecconi *et al.*[17] developed this work considerably by studying the solvate effect on the spin behaviour. In particular they observed sharp spin cross-over transitions between the quintet ($S = 2$) high-spin and singlet ($S = 0$) low-spin states in the range 150–230 K for $[Fe(dppen)_2Cl_2]\cdot n$solv (solv = Me_2CO, CH_2Cl_2 or $CHCl_3$) and $[Fe(dppen)_2Br_2]\cdot n Me_2CO$. For $[Fe(dppen)_2Cl_2]\cdot 2Me_2CO$ they found that the transition from high to low spin was essentially complete ($\mu_{eff} = 0.7\,\mu_B$) by 150 K, whereas for $[Fe(dppen)_2Br_2]\cdot 2Me_2CO$ the magnetic moment plateaued at relatively high values ($\mu_{eff} = 2.2\,\mu_B$), indicating that a fraction of the high-spin isomer was frozen in the lattice. In addition, single-crystal X-ray data were obtained for the high- (295 K) and low-spin (130 K) isomers of $[Fe(dppen)_2Cl_2]\cdot 2Me_2CO$ which confirmed the *trans* geometry of the complexes and revealed a mean decrease of 0.28 and 0.03 Å in the Fe–P and Fe–Cl distances respectively. This represents one of the largest structural changes observed for a spin cross-over system. The space group of the high-spin isomer was found to be $P2_1/a$. For the low-spin isomer the data were of lower quality and attempts to solve the data were made using both $P2_1/a$ and $P\bar{1}$, the former being utilised because of the difficulties caused by correlations in the lower-symmetry space group. König *et al.*[18] studied the Mössbauer spectra and X-ray powder diffraction patterns of $[Fe(dppen)_2Cl_2]\cdot 2Me_2CO$ and concluded that the spin-state transition was continuous (although relatively sharp) and that there was only a weak co-operative interaction between the individual complexes, leading to the conclusion that the high- and low-spin isomers were randomly distributed, effectively giving rise to a solid solution of the two components. In addition, they concluded that the

* *Non-SI units employed:* $\mu_B \approx 9.27 \times 10^{-24}$ J T^{-1}, bar = 10^5 Pa, eV $\approx 1.60 \times 10^{-19}$ J.

spin transition was associated with an order–disorder transition of the acetone molecules. McCusker *et al.*[19] investigated the pressure-induced spin cross-over in $[Fe(dppen)_2Cl_2]$ and $[Fe(dppen)_2Br_2]$ and found that the chloro complex underwent an abrupt first-order phase transition in the region 7–9 kbar, whilst the bromo complex underwent a gradual transition commencing at *ca.* 60 kbar. The higher pressure needed for the bromo complex was ascribed to the weaker ligand-field strength of Br^- compared to Cl^-. More recently, Wu *et al.*[20] have demonstrated the LIESST and reverse LIESST effect in $[Fe(dppen)_2Cl_2]\cdot CHCl_3$ at temperatures below 10 K. The room-temperature single-crystal structure of $[Fe(dppen)_2Br_2]$ has been reported,[21] but there appear to be no literature data for the acetone solvate in either the high- or low-spin form.

Therefore the aim of this work was to use XAFS to determine the local environment of the iron in the high- and low-spin isomers of $[Fe(dppen)_2Br_2]\cdot 2Me_2CO$ having checked that the values obtained from XAFS are reliable by use of the literature values[17] for $[Fe(dppen)_2Cl_2]\cdot 2Me_2CO$.

Experimental

Preparation of the complexes

The complexes were prepared according to literature methods;[16,17] an ethanolic solution (15 cm^3) of anhydrous iron(II) halide (1 mmol) (prepared from iron wire and hydrogen chloride or bromide at elevated temperatures) was refluxed with iron wire [to remove iron(III) impurities], filtered under nitrogen, and added to an acetone solution (40 cm^3) of dppen (2 mmol) (>98%, Strem Chemicals). The bright yellow precipitates (*ca.* 70–75% yield) were filtered under nitrogen, washed with ethanol (10 cm^3) and acetone (15 cm^3), dried by evacuation, and stored in a glove-box until required for the XAFS experiments. Both complexes gave satisfactory elemental analyses indicating the presence of acetone solvate molecules. The Fourier-transform IR spectra of both complexes contained a feature at 1713 cm^{-1} not present in the dppen spectra confirming the presence of acetone solvate [ν(C=O) for acetone is 1715.7 cm^{-1} in the solid, and 1739.8 cm^{-1} in the vapour[22]]. Therefore, in keeping with the earlier work,[17,18] it is assumed that there are two acetone solvate molecules for each iron complex, giving the formulae $[Fe(dppen)_2X_2]\cdot 2Me_2CO$ (X = Cl or Br).

XAFS Data collection and analysis

The complexes were diluted (*ca.* 1:1) and ground with graphite (99.999% Goodfellows, Cambridge), and made into 13 mm pressed discs before loading onto an APD DE204SL closed-cycle helium cryostat (base temperature *ca.* 10 K), mounted in an aluminium vacuum shroud, the details of which have been described elsewhere.[23]

The XAFS spectra were recorded in transmission mode (using Ar/He ion chambers) at the Daresbury Laboratory Synchrotron Radiation Source (SRS) operating at 2 GeV with average circulating currents of 150–260 mA. Iron K-edge data were collected on station 8.1 {using a Si[111] double-crystal monochromator operating at 70% harmonic rejection (*i.e.* 70% throughput) with a platinum focusing mirror} and station 9.2 (using a Si[220] double-crystal monochromator operating at 50% harmonic rejection). Bromine K-edge data were collected on the same sample at the same temperature using station 9.2. For the ambient-temperature spectra three or four data sets were recorded and averaged, whilst for the low-temperature data, one data set was found to be sufficient.

The iron K-edge data were calibrated using the first maximum in the first derivative of iron foil (7111.2 eV)[24] and the bromine K-edge data using the first maximum in the first derivative of the L_2 edge of gold foil (13 731 eV).[25] The XAFS data reduction was carried out using PAXAS[26] by fitting the pre-edge region using a quadratic polynomial, subtracting this from the data and approximating the atomic component of the post-edge region by high (typically sixth)-order polynomials or splines. Although it is normally possible to remove the low-*r* features in the Fourier transforms by careful choice of the post-edge background subtraction polynomial or spline parameters, in this case they were persistent and could not be removed using these standard methods. In recent years it has been noted that such features in the Fourier transforms may not be due to 'poor' background-subtraction techniques alone, but may actually arise from genuine low-frequency oscillations or sharp features in the post-edge region as a result of 'atomic' XAFS (AXAFS).[27] As these features are due to 'atomic' effects they will be most observable when the XAFS oscillations are relatively weak [as in this case for the ambient-temperature data (see below)], and their intensity should be constant between spectra at different temperatures for the same edge. This was observed for both the iron and bromine K-edge data confirming that the low-*r* features in these systems do indeed arise from AXAFS. In the case of the low-temperature data, these features were of acceptably low intensity, but in order to maintain consistency of data analysis all the spectra were treated in the same manner. Several prescriptions for removing low-*r* features have been advocated in the literature; these either rely on an iterative approach where the local scattering environment around the absorbing atom is relatively well defined, usually such as in model compounds,[27c–e,g] or by the use of 'zero crossing' methods from variable-temperature data.[28] In this work the latter approach is completely inappropriate as substantial structural modifications are expected on cooling, therefore a modified iterative approach was employed whereby the post-edge background subtraction was optimised (by minimising the low-*r* features), and an initial attempt at simulating the data in *k*-space was made. The areas of poor fit between the experiment and theory were noted and found to correspond to the features that gave rise to the low-*r* components in the Fourier transforms. The most pronounced mismatch was usually around 5–6 $Å^{-1}$ (*ca.* 95–135 eV after the edge), and such features have been observed before, and in the case of bromine K-edge XAFS assigned to 1s–3d two-electron excitations.[27c,d] The low-*r* features were then Fourier filtered and subtracted from the observed XAFS signal. The XAFS and Fourier transforms were then checked for the introduction of spurious features.

The XAFS spectral simulations were carried out using the curved-wave single- and multiple-scattering theory in EXCURV 92,[29] using a von-Barth ground state and a Hedin–Lundqvist exchange potential. The amplitude reduction factor due to shake-up and shake-off processes (AFAC) was set to 0.74 for Fe[30] and 0.82 for Br[31] as determined previously. In order to keep the number of refined independent parameters below $2\Delta k\Delta r/\pi$,[32] the co-ordination numbers were fixed at the crystallographic values unless otherwise stated.

Results and Discussion

The changes in the iron K-edge X-ray absorption near-edge structure (XANES) as a function of temperature for $[Fe(dppen)_2Cl_2]\cdot 2Me_2CO$ and $[Fe(dppen)_2Br_2]\cdot 2Me_2CO$ are shown in Fig 1. For $[Fe(dppen)_2Cl_2]\cdot 2Me_2CO$ the data are shown around the transition temperature, whereas for the bromo complex the data have been taken at 25 K intervals from ambient (298 K) to 25 K and then at 10 K. From these data it is clear that the transitions are reasonably sharp, and occur over a limited temperature range of 220–240 K for $[Fe(dppen)_2Cl_2]\cdot 2Me_2CO$ and 160–185 K for $[Fe(dppen)_2Br_2]\cdot 2Me_2CO$. These values are close to the values reported previously of *ca.* 230[17] and 240 K[18] for $[Fe(dppen)_2Cl_2]\cdot 2Me_2CO$ and *ca.* 190 K[17] for $[Fe(dppen)_2Br_2]\cdot 2Me_2CO$, indicating that the materials

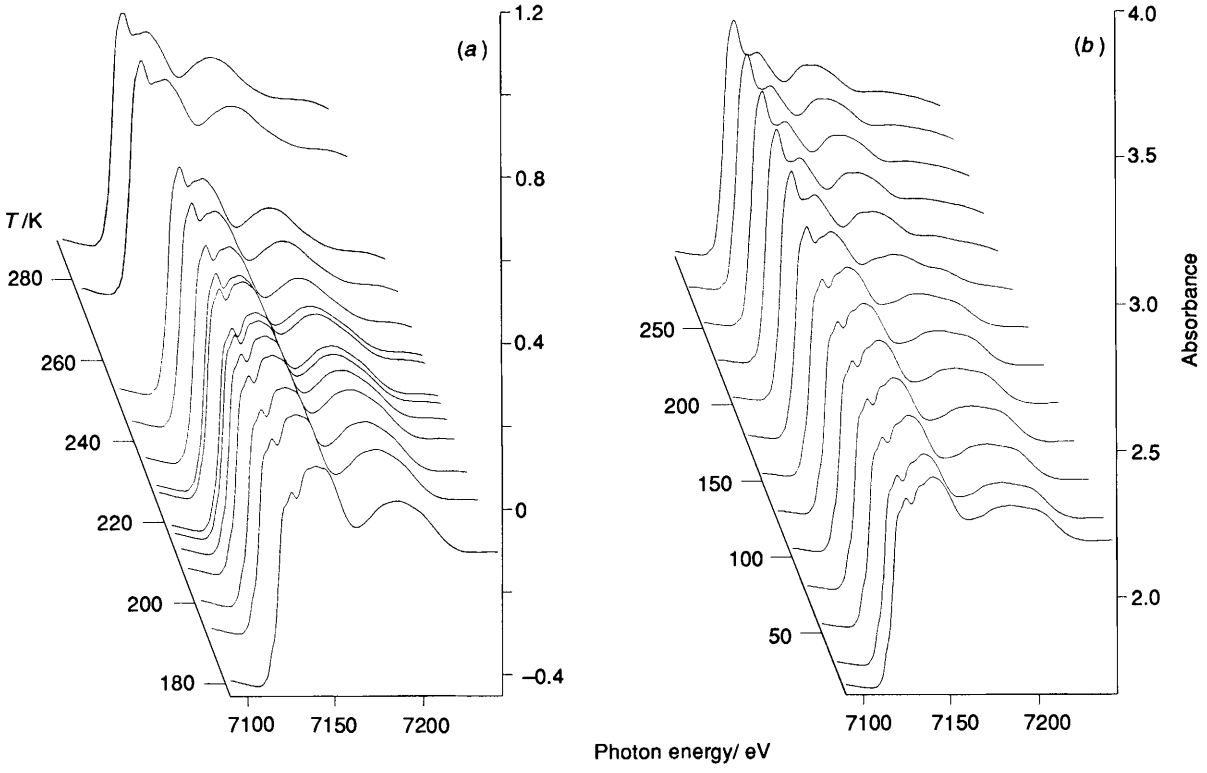

Fig. 1 Variable-temperature iron K-edge XANES spectra of (*a*) $[Fe(dppen)_2Cl_2]\cdot 2Me_2CO$ and (*b*) $[Fe(dppen)_2Br_2]\cdot 2Me_2CO$

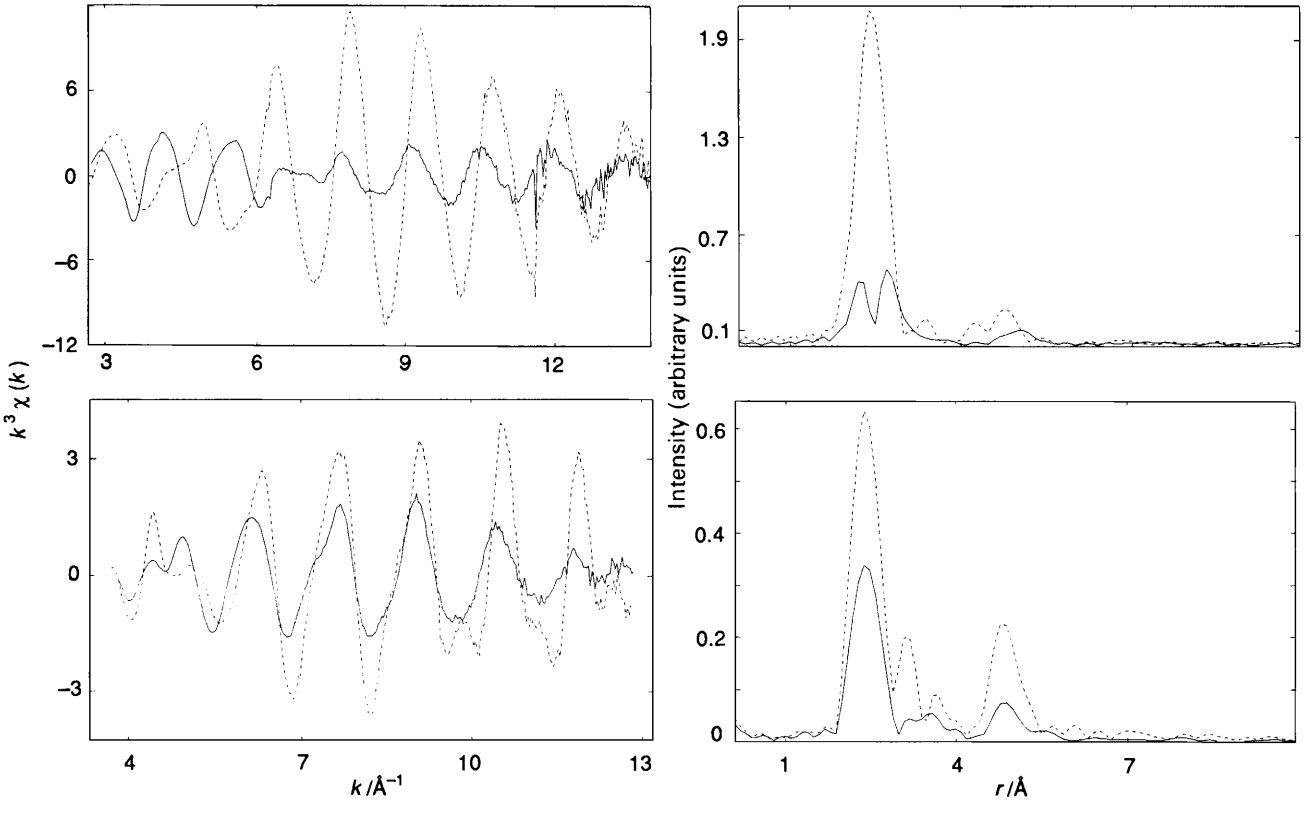

Fig. 2 Iron K-edge XAFS and Fourier transforms (top) and bromine K-edge XAFS and Fourier transforms (bottom) for $[Fe(dppen)_2Br_2]\cdot 2Me_2CO$ at 298 (——) and 10 K (- - -)

prepared in this work are behaving in a very similar fashion to that reported earlier. This therefore confirms that the acetone solvate remains in the lattice even when the samples are in a high-vacuum environment, as the unsolvated materials are known to behave very differently.[16,17]

The radical change in the XANES spectra of high- and low-spin iron(II) complexes has been identified as arising from the changes in geometric structure (*via* multiple scattering pathways) rather than a change in the electronic structure (*i.e.* $t_{2g}^4e_g^2 \longrightarrow t_{2g}^6e_g^0$),[10e,f] although the two are obviously highly correlated. The appearance of a shoulder at the foot of the edge in the low-temperature/low-spin spectra is indicative of a change in the electronic structure.

The changes in the broader XAFS oscillations in Fig. 1 are shown more extensively, together with their Fourier transforms, in Fig. 2 for the iron and bromine K-edge data from $[Fe(dppen)_2Br_2]\cdot 2Me_2CO$ at 298 and 10 K. A significant change in both the XAFS and Fourier transforms is expected

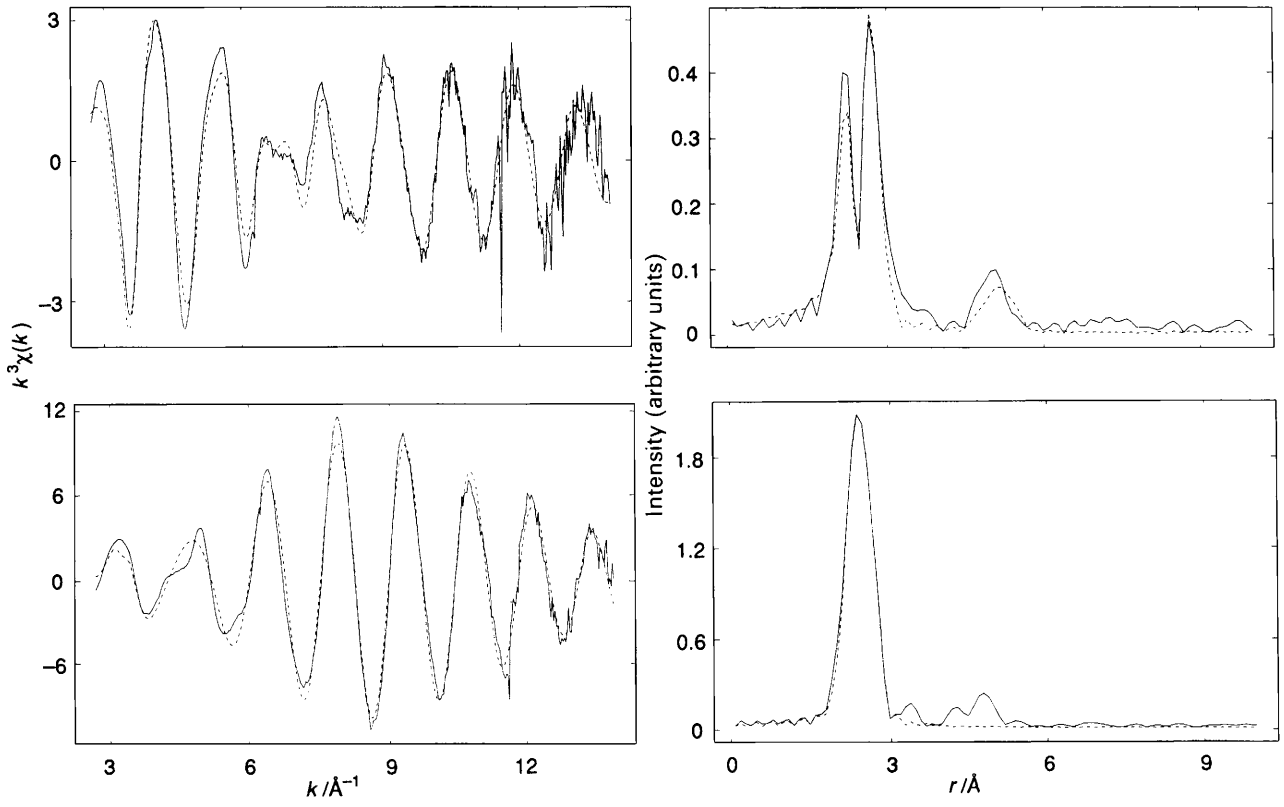

Fig. 3 Iron K-edge XAFS and Fourier transforms for $[Fe(dppen)_2Br_2]\cdot 2Me_2CO$ at 298 (top) and 10 K (bottom); ——, experimental data; -----, curved-wave theory

on going from 298 to 10 K due to the reduction in the thermal motion of the atoms. The change in the bromine K-edge data on going from 298 to 10 K is largely restricted to an intensity enhancement of all the features in the Fourier transform, indicating little structural modification is occurring and implying that it is essentially due to a reduction in the Debye–Waller factors. It should also be noted that the largest effect in the Fourier transform is for the shells at greatest distance, as these in general will be associated with low-frequency, high-amplitude, deformation modes, which will be significantly populated at all except low temperatures. The change in the XAFS amplitude for each shell is expected to be largest at high k, as the Debye–Waller term is k dependent (*i.e.* $e^{-2\sigma^2k^2}$). The difference between the 298 and 10 K data for the iron K-edge is much more dramatic and implies that there are structural changes as well as a reduction in the Debye–Waller factors. In this case there are two shells (Fe–P and Fe–Br) that are 'beating' against each other to a different extent in the high- (298 K) and low-spin (10 K) cases. This can be clearly seen as a 'node' in the 298 K data at *ca.* 7 Å^{-1}, but which is absent in the 10 K data. Unfortunately, the net result of these two factors is that at ambient temperatures the XAFS amplitudes are comparatively very weak and are therefore much more affected by the presence of monochromator glitches (*e.g.* at *ca.* 11.6 Å^{-1}) and AXAFS effects. Data recorded at 77 K for both the iron and bromine K-edges of $[Fe(dppen)_2Br_2]\cdot 2Me_2CO$ were essentially identical to those at 10 K, and the reversibility of the process was demonstrated by the fact that spectra collected at 298 K, before and after the cooling and warming cycle, were very similar, and the temperature cycling could be repeated.

The mean Fe–P and Fe–Cl bond lengths in $[Fe(dppen)_2Cl_2]\cdot 2Me_2CO$ at 298 and 130 K determined from the iron K-edge XAFS* are given in Table 1, together with the relevant X-ray diffraction data. The values obtained are in reasonable agreement with those from the single-crystal diffraction data and it is clear that, although there are slight discrepancies in the absolute values of the bond lengths determined by X-ray diffraction and XAFS, the *change* in the bond lengths (Δr) on going through the spin transition obtained from the two techniques are in very good agreement. The XAFS and Fourier transforms of data recorded at 77 K were essentially identical to those for 130 K. The reversibility of the structural changes was demonstrated by the fact that the spectrum recorded at 295 K after cooling and rewarming was essentially identical to the initial ambient-temperature spectrum, and that this process could be repeated. Therefore iron K-edge XAFS is able to provide reliable values of the change in the local iron environment between the high- and low-spin forms of $[Fe(dppen)_2Cl_2]\cdot 2Me_2CO$.

The XAFS and Fourier transforms, together with the best-fit simulations for $[Fe(dppen)_2Br_2]\cdot 2Me_2CO$ at 298 and 10 K, are shown in Fig. 3 for the iron K-edge data and Fig. 4 for the bromine K-edge data. The refined XAFS parameters and appropriate X-ray data are given in Table 1. As indicated earlier the greatest changes observed in the XAFS spectra between the high- and low-spin forms is in the iron K-edge spectra, with the changes in the bromine K-edge being more limited, implying that the significant structural changes are associated with the Fe–P interactions rather than the Fe–Br distances. This is to be expected from comparison with the data for $[Fe(dppen)_2Cl_2]\cdot 2Me_2CO$.[17] The agreement is good for the mean Fe–Br distances between the X-ray data[21] for unsolvated $[Fe(dppen)_2Br_2]$ [2.495(1) Å] and the XAFS data from both the iron K-edge [2.51(3) Å] and the bromine K-edge [2.48(3) Å] for the acetone solvate at 298 K.† In the case of the bromine K-edge data the Br···Br interaction was modelled using multiple-scattering techniques and it is clear from the values obtained

* The errors in interatomic distances arising from data collection and analysis have been estimated to be ±1.5% for well defined co-ordination shells.[33] This is usually an order of magnitude greater than the statistical errors reported by EXCURV 92.

† The Fe–Br and Br–Fe phase shifts have been shown previously to be satisfactory using EXCURV 90[34] and the original data[35] have been reanalysed using EXCURV 92 and the phase shifts remain satisfactory.

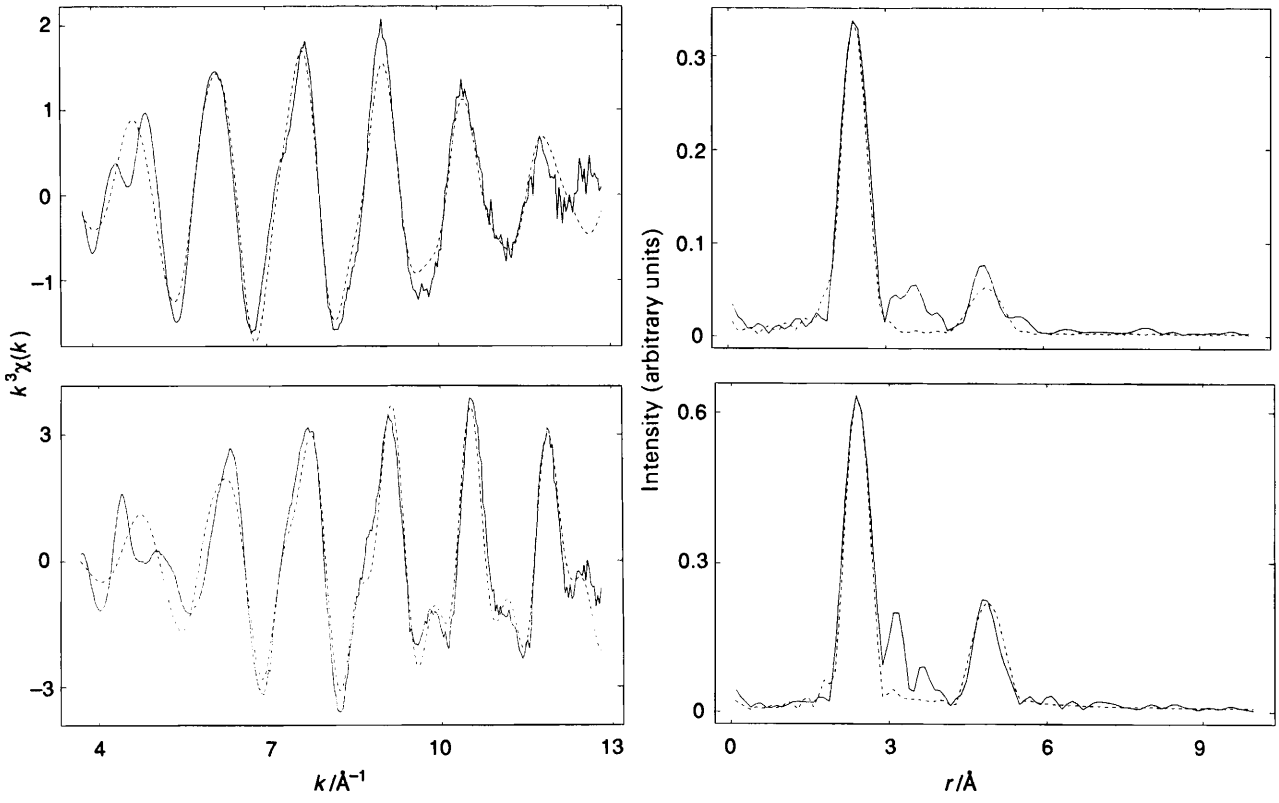

Fig. 4 Bromine K-edge XAFS and Fourier transforms for $[Fe(dppen)_2Br_2]\cdot 2Me_2CO$ at 298 (top) and 10 K (bottom); ——, experimental data; -----, curved-wave theory

Table 1 Refined XAFS parameters for $[Fe(dppen)_2Cl_2]\cdot 2Me_2CO$ and $[Fe(dppen)_2Br_2]\cdot 2Me_2CO$[a]

Single-crystal X-ray[b]	r(Fe–Cl)/Å		r(Fe–P)/Å				
$[Fe(dppen)_2Cl_2]$	2.347(1)		2.675(1) 2.532(1)				
$[Fe(dppen)_2Cl_2]\cdot 2Me_2CO$ 298 K	2.363(2)		2.592(2) 2.576(2)				
130 K	2.329(6)		2.312(8) 2.289(9)				
Δr[c]	0.03		0.28				
Iron K-edge XAFS[d]	r(Fe–Cl)[e]/Å	$2\sigma^2$(Fe–Cl)[f]/Å^2	r(Fe–P)/Å	$2\sigma^2$(Fe–P)/Å^2	E_f[g]/eV	R[h]	Fit index[i]
$[Fe(dppen)_2Cl_2]\cdot 2Me_2CO$ 298 K	2.335(5)	0.015	2.554(4)	0.017	−6.13	26.1	3.00
130 K	2.315(13)	0.001	2.273(7)	0.005	−5.38	18.4	1.24
Δr	0.02		0.28				
Single-crystal X-ray[j]	r(Fe–Br)/Å		r(Fe–P)/Å				
$[Fe(dppen)_2Br_2]$ 298 K	2.495(1)		2.674(2) 2.640(2)				
Iron K-edge XAFS[d]	r(Fe–Br)/Å	$2\sigma^2$(Fe–Br)/Å^2	r(Fe–P)/Å	$2\sigma^2$(Fe–P)/Å^2	E_f/eV	R	Fit index
$[Fe(dppen)_2Br_2]\cdot 2Me_2CO$ 298 K	2.507(2)	0.013	2.600(3)	0.018	−8.66	29.6	3.64
10 K	2.481(5)	0.004	2.310(3) × 2.7 2.613(9) × 1.7	0.003 0.007	−9.70	19.3	1.31
Δr	0.03		0.29				
Bromine K-edge XAFS[d]	r(Br–Fe)/Å	$2\sigma^2$(Fe–Br)/Å^2	r(Br···Br)/Å	$2\sigma^2$(Br···Br)/Å^2	E_f/eV	R	Fit index
$[Fe(dppen)_2Br_2]\cdot 2Me_2CO$ 298 K	2.482(3)	0.014	4.981(20)	0.029	−5.10	29.5	4.63
10 K	2.468(3)	0.005	4.940(8)	0.012	−9.64	33.4	5.08
Δr	0.01		0.04				

[a] Standard deviations in parentheses. [b] Ref. 17. [c] The difference in mean bond length between the solvated high- and low-spin isomers. [d] This work; all co-ordination numbers are the crystallographic values, except where stated otherwise. [e] Errors arising from data collection and analysis are estimated to be ± 1.5% for well defined co-ordination shells.[33] [f] $2\sigma^2$ is the Debye–Waller factor. [g] A single refined parameter to reflect differences in the theoretical and experimental Fermi levels. [h] $R = [\int|\chi^T - \chi^E|k^3dk/\int|\chi^E|k^3dk] \times 100\%$. [i] $\Sigma_i[(\chi_i^T - \chi_i^E)k_i^3]^2$. [j] Ref. 21.

that the Br–Fe–Br unit is approximately linear as the Br···Br interaction [4.98(7) Å] is very close to twice the Br–Fe distance [2.48(3) Å]. As noted above, the bromine K-edge data only change slightly on going from 298 to 10 K, and this is reflected in a slight decrease (0.01 Å) of the Br–Fe distance from 2.48(3) to 2.47(3) Å, with a substantial drop in Debye–Waller factor from 0.014 to 0.005 Å^2. The Br···Br interaction also shows a small shortening (0.04 Å) on going from high to low spin, again with a considerable drop in the Debye–Waller factor. (It is interesting that the Debye–Waller factor for the Br···Br interaction is approximately twice that of the Br–Fe interaction at both 298 and 10 K.) The change in the Fe–Br distances (0.03 Å) in iron

K-edge spectra from 298 to 10 K is similar to, but slightly larger than, that observed at the bromine K-edge, and of the same order of magnitude as observed for $[Fe(dppen)_2Cl_2]\cdot 2Me_2CO$. Although these differences in the Fe–Br bond lengths are very small and may not be statistically meaningful, the fact that they are observed for three different interactions (Fe–Br, Br–Fe and Br···Br) using two edges and that the spectra were collected from the same samples, under similar data-collection and analysis regimes, implies that there is a small but significant shortening (*ca.* 0.02 Å) of the Fe–Br interaction between the high- and low-spin isomers.

The features in the Fourier transforms of the bromine K-edge XAFS spectra between the Br–Fe and Br···Br shells are not readily fitted as they arise from a combination of Br···P and Br···C (both ethylene backbone and phenyl group) interactions. Fourier filtration of this portion of the Fourier transform was, however, able to confirm that it was made up of contributions from Br···P and Br···C shells. It is known from the crystal structure of $[Fe(dppen)_2Br_2]$[21] that there are four Br···P distances (3.482, 3.516, 3.737 and 3.811 Å) and 25 Br···C interactions (some of these are at very similar distances and some may involve multiple-scattering pathways) within the 5 Å local environment of Br.* In the case of $[Fe(dppen)_2Cl_2]$ there were four Cl···P distances in the unsolvated complex, as well as both the acetone-solvated high- and low-spin complexes.[17] In addition, there is also the problem of the residual high-spin fraction in the low-temperature spectra. Therefore it is believed that the poor quality of the fit at low k in the bromine K-edge spectra, is due to the inability to model this large number of interactions satisfactorily.

The changes observed in the iron K-edge spectra of $[Fe(dppen)_2Br_2]\cdot 2Me_2CO$ at 298 and 10 K are much more dramatic than for the bromine K-edge, and must therefore be due to changes in the Fe–P bond lengths. The mean Fe–P distance [2.60(3) Å] from the 298 K XAFS spectra of $[Fe(dppen)_2Br_2]\cdot 2Me_2CO$ is *ca.* 0.05 Å lower than the mean of those (2.65 Å) for $[Fe(dppen)_2Br_2]$ derived from the single-crystal X-ray data.[21] This apparent discrepancy may be real, or could be due to other causes; (*i*) it should be noted that there is a slight shortening (0.02 Å) of the mean Fe–P distance between the unsolvated and acetone-solvated $[Fe(dppen)_2Cl_2]$,[17] and (*ii*) there appears to be a systematic underestimate of the Fe–P (and Fe–Cl) bond lengths of 0.03 Å in the XAFS determination as compared to the X-ray data for $[Fe(dppen)_2Cl_2]\cdot 2Me_2CO$.[17]

The most significant changes in the Fourier transforms for the 298 and 10 K data are for the features at *ca.* 2.5 Å, which are associated with the Fe–P and Fe–Br interactions. In the 298 K (high-spin) data these are present as a pseudo-doublet of very low intensity (see Fig. 2), whereas in the 10 K data a single intense component is observed. This change is not due solely to a reduction in the Debye–Waller factors for the Fe–P and Fe–Br shells, but also to significant structural perturbations. In particular the mean Fe–P distance shortens by 0.29 Å on going from the high- [2.60(3) Å] to the low-spin [2.31(3) Å] isomer, whereas the Fe–Br distance is reduced by *ca.* 0.03 Å [2.51(3) to 2.48(3) Å]. These values are very similar to those obtained for $[Fe(dppen)_2Cl_2]\cdot 2Me_2CO$.[17] Although a reasonable fit to the iron K-edge data at 10 K could be obtained by assuming a complete conversion of high into low spin, it should be noted that Cecconi *et al.*[17] observed that a fraction of the high-spin form remained even at low temperatures for $[Fe(dppen)_2Br_2]\cdot 2Me_2CO$. Using their data and assuming[16] that μ_{eff} for $S = 2$ and $S = 0$ are 5.1 and 0.6 μ_B respectively, a value of approximately 20% of the high-spin form remaining at low temperatures is predicted. When a high-spin Fe–P distance was included the quality of the fit improved dramatically from R = 0.288 to 0.193, thus confirming that there is a high-spin fraction remaining in the sample. When the co-ordination numbers of the short (low-spin) and long (high-spin) Fe–P distances were refined a minimum was obtained at 2.7:1.7. Although this may indicate a larger high-spin fraction in this sample than reported earlier the minimum was fairly shallow, and it should be noted that it is very difficult to extract accurate co-ordination numbers from XAFS data, the normal precision level commonly accepted being *ca.* ± 1. The Fe–P distance obtained in this case [2.61(3) Å] is slightly longer than that observed for the original 298 K data [2.60(3) Å], but the statistical error is larger, and the difference is within the normal error margins and therefore probably not significant. Attempts to model the 10 K bromine K-edge data using two Br–Fe shells are complicated by the fact that the two distances are very similar, and by the presence of the multiple-scattering pathways, but when the Br–Fe shell was Fourier filtered the R factor actually got worse for two compared to a single Br–Fe interaction.

The additional feature at *ca.* 5 Å in the Fourier transform of the 298 K iron K-edge data is believed to be due to high-order multiple-scattering pathways involving Fe–Br–Fe–Br–Fe and *trans* Fe–P–Fe–P–Fe pathways shown. Although these have been invoked to explain multiple-scattering intensity enhancement in some systems[36] they cannot currently be modelled using EXCURV 92. Such features have also been observed[37] in the low-temperature nickel K-edge XAFS spectra of *cis*-$[Ni(dppe)Br_2]$ (dppe = $Ph_2PCH_2CH_2PPh_2$) and *trans*-$[Ni(PEt_3)_2Br_2]$ but which were absent in tetrahedral $[Ni(PPh_3)_2Br_2]$, confirming that they are due to multiple-scattering pathways in linear units, and indeed their presence in metal K-edge spectra could be used as a diagnostic tool for linearity in Y–M–X units. It should also be noted that the relative intensity of these features in the Fourier transforms of the iron K-edge data is much higher in the 298 than in the 10 K spectrum, which is surprising given the much reduced thermal motion in the low-temperature spectrum, but must be due to the foreshortening of the Fe–P and Fe–Br single scattering shells due to the differing beat effects. The fit to the iron K-edge 298 K data shown in Fig. 3 includes single-scattering contributions from four Fe–P and two Fe–Br distances at 5.28 and 4.92 Å respectively. Whilst these are quite close to twice the Fe–P (2.60 Å) and Fe–Br (2.51 Å) distances, it is clear that the backscattering phase and amplitudes are not correct, and these values should be treated with some caution, but do indicate that the premise that these features are due to an extended multiple-scattering pathway is probably correct. When the 298 K iron K-edge data were Fourier filtered over just the Fe–P and Fe–Br single-scattering shells a very good fit between experiment and theory was obtained. Attempts to fit the more distant features in the 10 K iron K-edge spectra were not successful, as these are of low intensity, and at the low temperatures involved the Fe···C contributions (28 up to 5.2 Å) become more important and very hard to model satisfactorily.

Conclusion

The data presented in this work confirm that K-edge XAFS is able to determine the structural changes occurring during spin cross-over in $[Fe(dppen)_2Cl_2]\cdot 2Me_2CO$ and $[Fe(dppen)_2Br_2]\cdot 2Me_2CO$. In the former case the changes observed in the mean Fe–P (0.28 Å) and Fe–Cl (0.02 Å) bond lengths in the iron K-edge

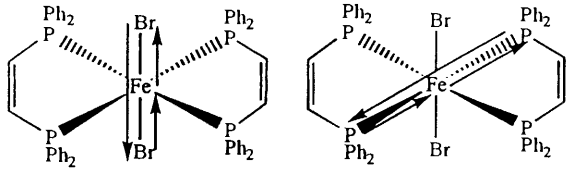

* Data obtained from the Chemical Database Service at Daresbury Laboratory using the CSSR and CRAD programs.

XAFS are in very good agreement with those derived from a single-crystal X-ray study.[17] For $[Fe(dppen)_2Br_2]\cdot 2Me_2CO$ the values of the mean Fe–P and Fe–Br bond lengths, and more importantly the change in these on going from the high- to the low-spin isomer, have been determined for the first time. In particular the mean Fe–P bond length shortens by 0.29 Å with a small (*ca.* 0.02 Å) but significant shortening of the mean Fe–Br interaction. These structural changes have been observed, despite the fact that there is a residual high-spin fraction in the sample, thus indicating the usefulness of XAFS techniques to the study of spin cross-over systems, where crystallographic data are not available. The reversibility of the spin cross-over process has also been demonstrated for both the chloro and bromo complexes.

Acknowledgements

The SERC/EPSRC is gratefully thanked for the award of an Advanced Fellowship, the granting of SRS beam time (Daresbury Laboratory Minor Grants 19/24, 20/118), equipment funds (GR/H 29117) and for access to the Chemical DataBase Service at Daresbury Laboratory. The Director of the Daresbury Laboratory is thanked for access to synchrotron and computing facilities. Professor C. D. Garner is thanked for access to some XAFS data and Dr. W. Levason for the gift of some dppen.

References

1 P. Gütlich, *Struct. Bonding (Berlin)*, 1981, **44**, 83; E. König, *Struct. Bonding (Berlin)*, 1991, **76**, 51.
2 P. Gütlich and A. Hauser, *Pure Appl. Chem.*, 1989, **61**, 849; J. Zarembowitch and O. Kahn, *Nouv. J. Chim*, 1991, **15**, 181; O. Kahn, J. Krober and C. Jay, *Adv. Mater.*, 1992, **4**, 718; C. Jay, F. Groliere, O. Kahn and J. Krober, *Mol. Cryst. Liq. Cryst. Sci. Tech. Sect. A*, 1993, **234**, 255.
3 P. Gütlich and A. Hauser, *Coord. Chem. Rev.*, 1990, **97**, 1; P. Gütlich, A. Hauser and H. Spiering, *Angew. Chem., Int. Ed. Engl.*, 1994, **33**, 2024.
4 A. W. Addison, S. Burman, C. G. Wahlgren, O. A. Rajan, T. M. Rowe and E. Sinn, *J. Chem. Soc., Dalton Trans.*, 1987, 2621.
5 C. Roux, J. Zarembowitch, B. Gallois, T. Granier and R. Claude, *Inorg. Chem.*, 1994, **33**, 2273.
6 E. König, *Prog. Inorg. Chem.*, 1987, **35**, 527.
7 B. Gallois, J. A. Real, C. Hauw and J. Zarembowitch, *Inorg. Chem.*, 1990, **29**, 1152; M. Konno and M. Mikami-kido, *Bull. Chem. Soc. Jpn.*, 1991, **64**, 339.
8 T. Granier, B. Gallois, J. Gaultier, J. A. Real and J. Zarembowitch, *Inorg. Chem.*, 1993, **32**, 5305.
9 *X-Ray Absorption*, eds. D. C. Koningsberger and R. Prins, Wiley, New York, 1988; B. K. Teo, *EXAFS: Basic Principles and Data Analysis*, Springer, Berlin, 1986.
10 (*a*) C. Cartier, P. Thuéry, M. Verdaguer, J. Zarembowitch and A. Michalowicz, *J. Phys. (Paris)*, 1986, **47**, C8-563; (*b*) C. Cartier and M. Verdaguer, *J. Chim. Phys. Phys.-Chim. Biol.*, 1989, **86**, 1607; (*c*) C. Cartier dit Moulin, P. Sainctavit and V. Briois, *Jpn. J. Appl. Phys.*, 1993, **32 (Suppl. 32–2)**, 38; (*d*) N. V. Bausk, S. B. Erenburg, L. N. Mazalov, L. G. Lavrenova and V. N. Ikorskii, *J. Struct. Chem. (Engl. Transl.)*, 1994, **35**, 509; (*e*) V. Briois, C. Cartier dit Moulin, P. Sainctavit, C. Brouder and A. M. Flank, *J. Am. Chem. Soc.*, 1995, **117**, 1019; (*f*) L. X. Chen, Z. Y. Wang, J. K. Burdett, P. A. Montano and J. R. Norris, *J. Phys. Chem.*, 1995, **99**, 7958.
11 H. Oyanagi, T. Iizuka, T. Matsushita, S. Saigo, R. Makino, Y. Ishimura and T. Ishiguro, *J. Phys. Soc. Jpn.*, 1987, **56**, 3381; H. Winkler, A. Sawaryn, A. X. Trautwein, C. Hermes and H. Toftlund, *Recl. Trav. Chim. Pays-Bas*, 1987, **106**, 323; H. Oyanagi, T. Iizuka, T. Matsushita, S. Saigo, R. Makino and Y. Ishimura, *Biophys. Synchrotron Rad.*, 1987, **2**, 99; H. Winkler, A. Sawaryn, A. X. Trautwein, A. S. Yousif, C. Hermes, H. Toftlund and R. H. Herber, *Hyperfine Interact.*, 1988, **42**, 921; Z. R. Korszun, G. Bunker, S. Khalid, W. R. Scheidt, M. A. Cusanovich and T. E. Meyer, *Biochemistry*, 1989, **28**, 1513.
12 C. Butzlaff, E. Bill, W. Meyer, H. Winkler, A. X. Trautwein, T. Beissel and K. Weighardt, *Hyperfine Interact.*, 1994, **90**, 453.
13 J. Zarembowitch, P. Thuéry, A. Dworkin and A. Michalowicz, *J. Chem. Res.*, 1987, (*S*) 146; P. Thuéry. J. Zarembowitch, A. Michalowicz and O. Kahn, *Inorg. Chem.*, 1987, **26**, 851; V. Briois, C. Cartier, M. Momenteau, P. Maillard, J. Zarembowitch, E. Dartyge, A. Fontaine, G. Tourillon, P. Thuéry and M. Verdaguer, *J. Chim. Phys. Phys.-Chim. Biol.*, 1989, **86**, 1623; C. Roux, J. Zarembowitch, J. P. Itié, M. Verdaguer, E. Dartyge, A. Fontaine and H. Tolentino, *Inorg. Chem.*, 1991, **30**, 3174; J. Zarembowitch, *Nouv. J. Chim.*, 1992, **16**, 255; T. Arunarkavalli, G. U. Kulkarni and C. N. R. Rao, *J. Solid State Chem.*, 1993, **107**, 299.
14 C. Cartier dit Moulin, P. Rudolf, A. M. Flank and C. T. Chen, *J. Phys. Chem.*, 1992, **96**, 6196; C. Cartier dit Moulin, A. M. Flank, P. Rudolf and C. T. Chen, *Jpn. J. Appl. Phys.*, 1993, **32 (Suppl. 32–2)**, 308.
15 M. Abbate, J. C. Fuggle, A. Fujimori, L. H. Tjeng, C. T. Chen, R. Potze, G. A. Sawatzky, H. Eisaki and S. Uchida, *Phys. Rev. B*, 1993, **47**, 16124.
16 W. Levason, C. A. McAuliffe, M. M. Khan and S. M. Nelson, *J. Chem. Soc., Dalton Trans.*, 1975, 1778.
17 F. Cecconi, M. di Vaira, S. Midollini, A. Orlandini and L. Sacconi, *Inorg. Chem.*, 1981, **20**, 3423.
18 E. König, G. Ritter, S. K. Kulshreshtha, J. Waigel and L. Sacconi, *Inorg. Chem.*, 1984, **23**, 1241.
19 J. K. McCusker, M. Zvagulis, H. G. Drickamer and D. N. Hendrickson, *Inorg. Chem.*, 1989, **28**, 1380.
20 C. C. J. Wu, K. M. Sena, D. N. Hendrickson, J. Jung and P. Gütlich, *Abstr. Pap. Am. Chem. Soc. Mtg.*, 1994, **207(Pt1)**, 392-INOR.
21 F. Cecconi, M. Di Vaira and L. Sacconi, *Cryst. Struct. Commun.*, 1981, **10**, 1523.
22 *Sprouse Collection of Infrared Spectra IV*, ed. D. L. Hansen, Elsevier, New York, 1990.
23 I. R. Beattie, N. Binsted, W. Levason. J. S. Ogden, M. D. Spicer and N. A. Young, *High Temp. Sci.*, 1989, **26**, 71.
24 C. Cartier, M. Momenteau, E. Dartyge, A. Fontaine, G. Tourillon, A. Michalowicz and M. Verdaguer, *J. Chem. Soc., Dalton Trans.*, 1992, 609.
25 W. Levason, J. S. Ogden, M. D. Spicer and N. A. Young, *J. Chem. Soc., Dalton Trans.*, 1990, 349.
26 N. Binsted, PAXAS, Program for the Analysis of X-Ray Absorption Spectra, University of Southampton, 1988.
27 See, for example, (*a*) B. W. Holland, J. B. Pendry, R. F. Pettifer and J. Bordas, *J. Phys. C.*, 1978, **11**, 633; (*b*) J. W. Cook and D. E. Sayers, *J. Appl. Phys.*, 1981, **52**, 5024; (*c*) G. G. Li, F. Bridges and G. S. Brown, *Phys. Rev. Lett.*, 1992, **68**, 1609; (*d*) A. I. Frenkel, E. A. Stern, M. Qian and M. Newville, *Phys. Rev. B*, 1993, **48**, 12449, (*e*) J. J. Rehr, C. H. Booth, F. Bridges and S. I. Zabinsky, *Phys. Rev. B*, 1994, **49**, 12347; (*f*) J. J. Rehr, S. I. Zabinsky, A. Ankudinov and R. C. Albers, *Physica B*, 1995, **208**, **209**, 23; (*g*) F. Bridges, C. H. Booth and G. G. Li, *Physica B*, 1995, **208**, **209**, 121.
28 E. A. Stern, P. Livinš and Z. Zhang, *Phys. Rev. B*, 1991, **43**, 8850; M. Newville, P. Livinš, Y. Yacoby, J. J. Rehr and E. A. Stern, *Phys. Rev. B*, 1993, **47**, 14126.
29 N. Binsted, J. W. Campbell, S. J. Gurman and P. C. Stephenson, Daresbury Laboratory EXCURV 92 program, 1991; S. J. Gurman, N. Binsted and I. Ross, *J. Phys. C*, 1984, **17**, 143; 1986, **19**, 1845.
30 I. R. Beattie, P. J. Jones and N. A. Young, *J. Am. Chem. Soc.*, 1992, **114**, 6146.
31 W. Levason, J. S. Ogden, M. D. Spicer and N. A. Young, *J. Am. Chem. Soc.*, 1990, **112**, 1019.
32 *X-Ray Absorption Fine Structure*, ed. S. S. Hasnain, Ellis Horwood, Chichester, 1991, ch. 195, p. 751.
33 J. M. Corker, J. Evans, H. Leach and W. Levason, *J. Chem. Soc., Chem. Commun.*, 1989, 181.
34 A. K. Powell, J. M. Charnock, A. C. Flood, C. D. Garner, M. J. Ware and W. Clegg, *J. Chem. Soc., Dalton Trans.*, 1992, 203.
35 C. D. Garner, University of Manchester, personal communication.
36 P. A. O'Day, J. J. Rehr, S. I. Zabinsky and G. E. Brown, *J. Am. Chem. Soc.*, 1994, **116**, 2938.
37 N. A. Young, unpublished work.

Received 9*th October* 1995; *Paper* 5/06653K